CHAPTER

3.5 MICROSTRUCTURE AND OXIDATION BEHAVIOR OF ATMOSPHERIC PLASMA-SPRAYED THERMAL BARRIER COATINGS

Ali Avci[1], **Aysegul A. Eker**[1], **Bulent Eker**[2]
Yildiz Technical University, Istanbul, Turkey[1]; *Namik Kemal University, Tekirdag, Turkey*[2]

1. INTRODUCTION

Technological developments create harsh environmental operating conditions such as high temperature, mechanical loading, oxidation, corrosion, and erosion. Metals may not provide the necessary properties for operating conditions in which a ceramic (oxide and nitride) is deposited on a substrate as a protective layer. Ceramic materials have been used in many high-temperature applications as refractors owing to their high melting temperature. These refractor ceramic materials need to have basic properties, phase stability at a high temperature, a high thermal expansion coefficient, and low thermal conductivity. Elevated pressure turbine blades are one of the biggest challenges engineers need to overcome. Today, they can resist gas temperatures higher than the melting point of the underlying substrate metal. This phenomenon would not have been possible if it were not for the ultimate strength of superalloys and the development of coatings. Also, the isolation of metallic substrates provides the ability to work in higher temperature close to the melting point of the substrate. Thermal barrier coatings (TBCs) were first used for aerospace applications. Calcia-stabilized zirconia and frit enamels were deposited onto the exhaust nozzle of a manned rocket in the 1960s by the National Advisory Committee for Aeronautics.

In the 1950s, turbine inlet temperatures were about 800°C. Currently, inlet temperatures exceed 1500°C. TBCs reduce surface temperature to more than 100°C. The turbine blade surface first used deposited layered protective coatings in the 1960s, and then the application was improved. Advanced protective coatings were developed for use in engine and land-based turbine blades, marine gas turbines, and diesel engines. Typical examples are turbine engine components, turbine blades, combustion chambers, duct, and nozzle guide vanes. Gas turbine inlet temperatures can surpass the melting temperatures of superalloy substrates. Advanced air cooling systems in association with TBCs can reduce substrate temperatures. However, instead of these uneconomic cooling systems, TBCs are preferred. To improve gas turbine engine efficiency, usually the temperature of the combustor and

Exergetic, Energetic and Environmental Dimensions. http://dx.doi.org/10.1016/B978-0-12-813734-5.00045-7
Copyright © 2018 Elsevier Inc. All rights reserved.

turbine engine should be as high as possible. TBCs can resolve the problem of the turbine temperature because it needs less air cooling; this results in an increase in the performance of TBCs in the turbine engine and service lifetime and decrease the fuel consumption of engines. According to previous studies, using a TBC can save up to 150 million liters of fuel per year for 1000 aircraft. At a high temperature, the structural material and most critical components are at a risk of degradation. Thermal protection is necessary to increase the service lifetime and durability. TBCs are applied to significant components such as the gas turbine and aeronautic engine parts at high temperatures. Gas turbine engines, which are used to impel aircraft and generate electricity, are Carnot engines whose efficiency depends on the temperature of the gas turbine. Temperatures of gas turbine components are 320°C for compressors, 1300°C for combustors, and 1050°C for turbines. TBC systems consist of multiple layers to obtain desirable properties from TBCs under these harsh condition [1,2]. TBCs are also employed on the piston surface, which is considered a solution to reduce unburned hydrocarbon emissions produced by incomplete combustion with respect to the crack volume when engines start, and which decrease thermal conductivity and increase unburned charge oxidation.

Yttria-stabilized zirconia (YSZ) is the most widely applied TBC material because of its high thermal shock resistance, high oxidation, and thermal fatigue resistance up to 1150°C. TBCs are usually deposited by two methods: plasma spraying and electron beam physical vapor deposition (EBPVD). They can also be deposited by high-velocity oxygen fuel (HVOF) spraying for processes such as blade tip wear and erosion protection. HVOF is commonly applied to deposit aluminide, the bond coat powders MCrAlY, WC/Co, and Cr_2C_3/NiCr, and dense cermet. Residual stress can occur as the result of a ceramic TBC and a metallic substrate having different coefficients of thermal expansion. It was reported that TBCs increased in operating temperature and turbine efficiency by 8% and decreased fuel consumption by 15%−20%. TBCs are also used in gas turbine engines to obtain better performance by increasing the gas temperature and reducing the amount of cooling air. However, an increase in the operating temperature leads to enhanced thermal fatigue and a severe decrease in the operating time because of the rapid oxidation of the bond coat. Turbine components are all made of ceramic; however, the desired features and productivity of turbines have not yet been obtained owing to thermal shock and cracks. Increases in the gas turbine inlet temperature not only improve the TBC's microstructure but allow the development of new and alternative TBCs materials. Studies have focused on YSZ/$La_2Zr_2O_7$ composite or YSZ/CeO_2-layered composite TBCs to obtain better oxidation and thermal shock resistance. Currently, ceramic materials are used as TBCs such as YSZ, Al_2O_3, mullite, CaO-MgO + ZrO_2, CeO_2 + YSZ, and Y_2O_3 + HfO_2 commercial gas turbine determinate components. The turbine inlet temperature is about 1500 to 1600°C in military or commercial aircraft; this inlet temperature is anticipated to reach 1750°C. Regarding the development of substrates, TBC materials and cooling systems might increase the gas turbine inlet temperature which provides a large number of thermal cycling and the most efficient gas turbine. Last year's 1−1.5 million kilograms of YSZ was atmospheric plasma-spray (APS) deposited onto gas turbine components. TBCs are significant components in gas turbine engines. Because the processing temperatures are about 90% of the melting point of the underlying superalloys, any TBC failure such as spallation, oxidation, or corrosion can put an engine at risk. TBCs can lead to increased numbers of takeoffs and landing in gas turbines [3−7].

2. THERMAL BARRIER COATINGS

The selection of materials related to the properties and microstructure of powders can lead to the prolonged service life of TBC. TBCs improve engine endurance and create less internal friction, decreased erosion and corrosion, lower noise, and decreased exhaust emissions.

2.1 MATERIALS

The selection of materials for TBCs needs specific requirements such as thermal expansion coefficient adaptation between the substrate and the ceramic top coat, a high melting point, and low thermal conductivity. There is no phase transformation at operating temperature (room temperature), good oxidation, and erosion resistance. It should also provide favorable adhesion, low sintering of the porous structure, thermal stability, and chemical stability. The number of applied TBC materials is limited. A ceramic material that includes the thermal conductivity and thermal expansion coefficient appears to be the most significant properties for the selection of a TBC material. The selection of material in the TBC system is the key factor in order to get desired performance, low emissions and low fuel consumption in engines. In addition to YSZ, Al_2O_3, TiO_2, mullite, $Y_2O_3 + HfO_2$, CaO/MgO + $ZrOAl_2O_3$, and $CeOAl_2O_3$ + YSZ, ceramic powders were evaluated as TBC materials. Advantages and disadvantages of the TBC materials are given in Table 1. The most common TBC material, YSZ, underwent destructive failures by sintering and phase transformation. Sintering causes microstructural changes and phase transformation leads to a change in volume. As a result, both can cause destructive failure and decrease thermal cycling in TBCs. $La_2Hf_2O_7$, $Gd_2Zr_2O_7$, and $Nd_2Zr_2O_7$ ceramic materials are also used as a TBC because of their high thermal stability and low thermal conductivity.

Fig. 1 shows that the thermal expansion coefficients of Al_2O_3, MgO, and ZrO_2 were closer to the nickel super alloy substrate but YSZ was preferred because of its lower thermal conductivity. The thermal conductivity of TBC materials can change between 1 and 30 $m^{-1}\,K^{-1}$, depending on the processing technology and parameters. APS YSZ has the lowest thermal conductivity: 1.2−2 $m^{-1}\,K^{-1}$. Decreasing the surface temperature using TBCs provides many advantages including decreasing the rate of heat transfer through the substrate, decreasing the risk of creep, and increasing productivity [8,9].

2.1.1 Yttria-Stabilized Zirconia

The most common ceramic for top coats is YSZ; it contains 7 wt% Y_2O_3-ZrO_2 owing to its outstanding properties, such as a high coefficient of thermal expansion (10.0−10^{-6}/K), high melting point at less than 2680°C, low thermal conductivity, phase stability at high temperature, low sintering rate, low elastic modulus of 40 GPa, proven manufacturing capability to be deposited with a specific composition, and high operating time. Although pure zirconia (ZrO_2) has other main physical and chemical properties, its high mechanical properties, such as chemical stability, ionic conductivity, low thermal conductivity, and high melting point, make it attractive as an engineering material for oxide fuel cells, biomaterials, oxygen sensors, and synthetic diamonds. Nevertheless, its use is mainly limited to refractory applications and engineering ceramics. Typically the top coat is metastable tetragonal (t′) structured zirconia because pure zirconia reveals the phase transformation. Fig. 2 illustrates the polymorphic crystal structures of zirconia: monoclinic, tetragonal, and cubic. The monoclinic polymorph has been transformed to tetragonal phase because of martensitic transformation around 1170°C.

Table 1 Advantages and Disadvantages of Thermal Barrier Coating Materials

Materials	Advantage	Disadvantage
ZrO_2 7−8 wt% Y_2O_3	High thermal expansion coefficient High thermal shock resistance Low thermal conductivity	Phase transformation at 1170°C Sintering above 1200°C Corrosion and oxygen diffusion
Mullite ($3Al_2O_3$ $2SiO_2$)	Low thermal conductivity High corrosion resistance Low oxygen diffusion Good High thermal shock resistance	Crystallization (700−1000°C) Very low thermal expansion coefficient
Alumina (Al_2O_3)	High corrosion resistance Dense microstructure High mechanical properties Low oxygen diffusion	Phase transformation above 1000°C Very low thermal expansion High thermal conductivity coefficient
CeO_2 + YSZ	Low thermal conductivity High thermal expansion coefficient Lower phase transformation from monoclinic to tetragonal High thermal shock resistance	High sintering rate CeO_2 precipitation above 1100°C Loss of CeO_2 during spraying
$La_2Zr_2O_7$	Low thermal conductivity Ultrahigh thermal stability Low sintering rate and low oxygen Diffusion	Low thermal expansion coefficient
$La_2Ce_2O_7$	Low thermal conductivity Ultrahigh thermal stability High thermal expansion coefficient High corrosion resistance	Reduces CeO_2 during coating High sintering ratio above 1250°C
Silicates	Cheap and available High corrosion resistance	Very low thermal expansion Coefficient

Adapted from Cao XQ, Vassen R, Stoever D. Ceramic materials for thermal barrier coatings. Journal of the European Ceramic Society 2004;24(1):1−10. http://doi.org/10.1016/S0955-2219(03)00129-8.

The tetragonal phase can be stable at room temperature. The final phase transformation took place at 2370°C, at which the tetragonal phase transformed to a cubic phase. The tetragonal to monoclinic phase transformation (t: ZrO_2—m: ZrO_2) took place by martensitic transformation, which was accomplished by the movement of atoms within the lattice without breaking bonds. The monoclinic−tetragonal transformation led to an increase in volume in the structure by about 3%−5%, which resulted in cracking, the creation of tensile stress, catastrophic fracture, and spallation failure.

To keep the tetragonal phase of transformation from going into a monoclinic phase, CaO, MgO, Y_2O_3, and CeO_2 were added to zirconia. This permitted metastable tetragonal ZrO_2 (t′) to protect stability at a low temperature in the form of an equiaxed polycrystalline aggregate and it did not transform the monoclinic phase. The Y_2O_3-stabilized ZrO_2 YSZ demonstrated the unusual properties of high thermal stability, high thermal expansion coefficient, low thermal conductivity, and high fracture toughness. Fracture toughness in the TBCs was significant not only for resisting impacts and erosion but also for spallation. The thermal expansion coefficients of Al_2O_3 and MgO ceramics were close to those of superalloy substrates such as YSZ ceramic; however, their thermal conductivity was

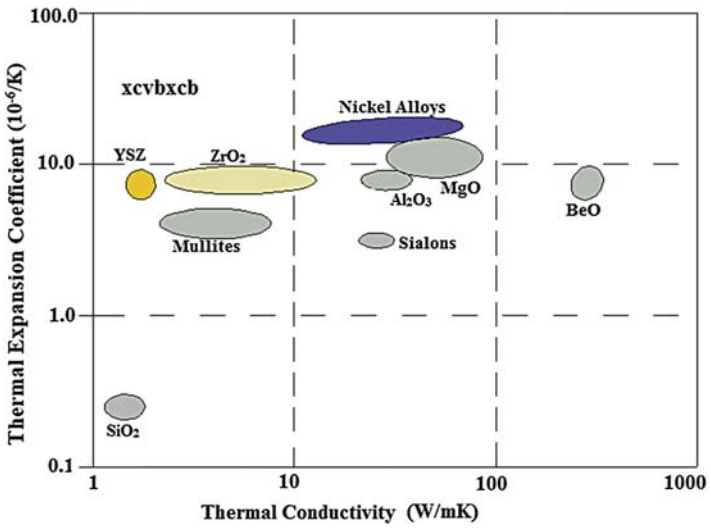

FIGURE 1

Thermal conductivity and thermal expansion coefficient of thermal barrier coating materials. *YSZ*, yttria-stabilized zirconia.

From Karaoglanli AC, Ogawa K, Türk A, Ozdemir I. Thermal shock and cycling behavior of thermal barrier coatings (TBCs) used in gas turbines. Progress in Gas Turbine Performance 2013, 237–60. http://dx.doi.org/org/10.5772/54412.

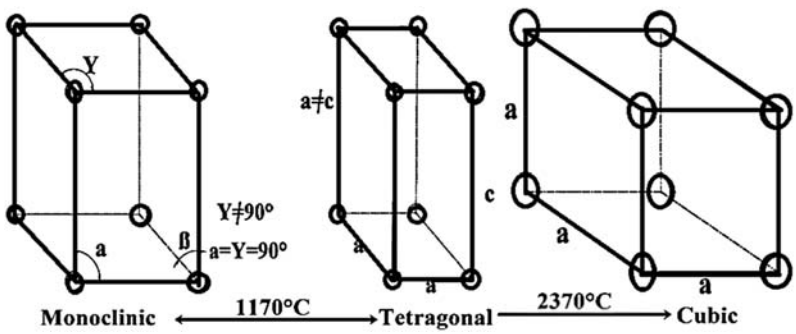

FIGURE 2

Phase transformation of zirconia.

higher than YSZ. Resistance to oxidation and to hot corrosion for YSZ was higher than for Al_2O_3 and MgO. Phase transformation at 850°C to 1000°C from tetragonal phase to monoclinic phase is shown in Fig. 3; it resembled a martensitic transformation in steel. According to the diagram, quick cooling rates followed the metastable nonequilibrium tetragonal phase [10]. The solid solutions diagram of Yttria (7 wt%) ZrO_2 shows better phase stability at variable temperature.

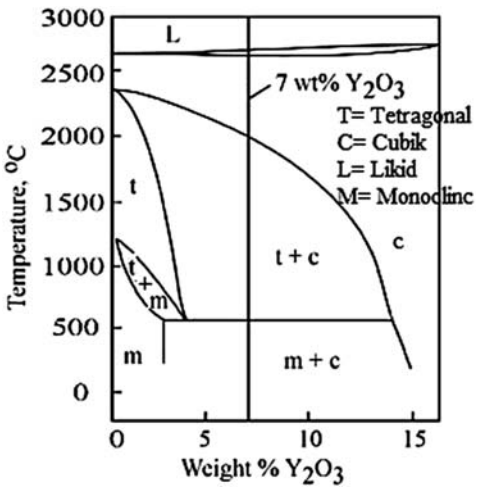

FIGURE 3

Yttria (7 wt%) ZrO_2 phase distribution at various temperatures.

To prevent the destructive monoclinic to tetragonal phase transformation that could cause mechanical damage to zirconia, 7% yttria with zirconia is necessary; however, it also decreases thermal conductivity by creating point defects that scatter phonons. YSZ is the most commonly use material for plasma-sprayed TBCs; it is produced as a tetragonal metastable polymorph containing around 6%−8% weight of yttria, which is stabilized into its cubic form by a high content of yttria. The monoclinic YSZ formed with a low yttria content reveals a martensitic transformation to a tetragonal phase around 1170°C, and it is stable only at low temperatures. The monoclinic−tetragonal transformation leads to increased volume in the structure by about 3%−5% that may result in cracking and spallation failure. Monoclinic phase in coatings should be avoided for this phase transformation. The manufacturing method and places of operation is important for determining the yttrium oxide rate in YSZ [9]. YSZ leads to oxygen diffusion through the bond coat because of its porous microstructure; correspondingly, thermally grown oxide (TGO) is formed on the bond coat. A thin TGO layer causes spallation and protects the substrate from oxidation. In the literature, a thicker dense alumina layer was coated on YSZ to avoid oxygen diffusion through the bond coat [5,11−15].

2.1.2 Lanthanum Zirconate

Lanthanum zirconate (LZ) ($La_2Zr_2O_7$) is a promising alternative TBC material that has a high melting point, low thermal conductivity, and low oxygen diffusion. It also has low toughness and a low thermal expansion coefficient. The production of LZ is slow and it is hard to find commercially. LZ TBCs can have phase stability up to 1400°C without an Al NiCrAlY bond coating. LZ has demonstrated spallation under 1000°C owing to the La_2O_3 phase that occurs as a reaction between the bond coat and LZ. Although LZ has lower thermal conductivity than does YSZ, it has lower thermal cycling resistance owing to its low toughness and thermal expansion coefficient [16]. In addition, 20% wt% $Y_3Al_5O_{12}$ or 20 wt% $BaTiO_3$ can increased LZ toughness, and adding CeO_2 can reduce thermal conductivity and improve sintering behavior [5,12,14].

2.1.3 Alumina (Al_2O_3)

Alumina (Al_2O_3) has chemical stability, mechanical resistance, accessibility and low oxidation because of its dense microstructure. Fig. 1 shows that Al_2O_3 and the superalloy substrate had a close thermal expansion coefficient. Because of its high thermal conductivity and phase instability, Al_2O_3 is not used alone as a TBC material. Al_2O_3 is usually added to existing TBC powders. In this way, oxidation and erosion resistance can be improved, toughness and elastic modulus can increase, and the bond strength and hardness can increase as well. In the process of plasma spraying the coating, an unstable phase can occur, such as γ- and δ-Al_2O_3. These unstable phases will transform to stable α-Al_2O_3 during thermal cycling. As a result, the coating volume may decrease about 15%, owing to a microcrack in the structure. α-Al_2O_3 can be stabilized by adding Cr_2O_3, TiO_2, or Fe_2O_3 transition metal oxides Studies showed that YSZ and Al_2O_3 composite coatings decrease crack formation, add high mechanical properties, and reduce the thermal mismatch between the top coat and bond coat [5,12,13,15,17–21].

2.1.4 Cerium Oxide

CeO_2 has low thermal conductivity and a high thermal expansion coefficient compared with YSZ. CeO_2 + YSZ (CYSZ) has a better thermal cycle and lower thermal conductivity than YSZ because the added ceria makes zirconia more stable at a high temperature. Thus, CYSZ is an alternative material to TBC. Adding ceria to a YSZ coating creates less of a phase transformation of YSZ from monoclinic to tetragonal. CYSZ has less thermal conductivity and also less bond coat stress. CeO_3 is transformed into CeO_2 in CYSZ because the hardness is reduced [4,8,10,22,23].

2.1.5 Mullite

Mullite ($3Al_2O_32SiO_2$) has been used a TBC materials because of its promising properties, such as low density, chemical stability under aggressive working conditions, low thermal conductivity, high temperature resistance, and good creep resistance. Consisting of SiO_2 and Al_2O_3, mullite has a low expansion coefficient and low thermal conductivity. During the plasma spray process, mullite is formed in the amorphous phase as a result of the high cooling speed of molten mullite. It can preserve stability and thermal conductivity above 1500°C. Mullite has higher thermal cycling than YSZ below 1000°C. However, above 1000°C, thermal cycling is reduced because the volume changes. Mullite is an excellent alternative TBC material in diesel combustion engines at lower temperatures [12,20,23].

2.2 STRUCTURE OF THERMAL BARRIER COATINGS

Conventional thermal coatings basically consist of a multilayer; a ceramic top coat, a metallic bond coat, substrate, and thermally grown oxide (Fig. 4). They are a ceramic insulation layer (YSZ), which is a main layer to protect the system against environmental and heat effects; it has low thermal conductivity that reduces the temperature of the metal.

The bond coat can balance thermal expansion coefficients between the ceramic top coat and the metal substrate. MCrAlY-based bond coats are used as oxidation layers; they provide adhesion between the metal substrate and the ceramic top coat. MCrAlY coatings (M = Ni, Co, or Ni) have been commonly applied since the 1970s as bond coats on superalloys to protect substrates against oxidation [17]. TGO is an oxide layer that occurs during thermal cycling at the interface of a ceramic top coat superalloy metallic substrate. Nickel-based superalloys are generally used as a substrate, which is

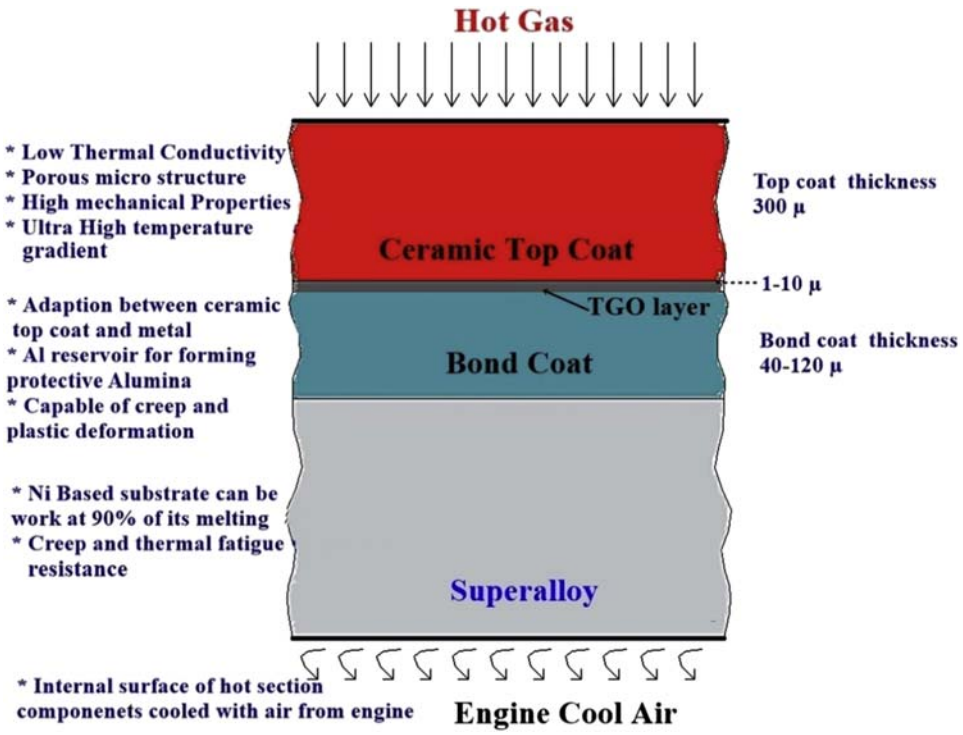

FIGURE 4

Thermal barrier coating system with a yttria-stabilized zirconia top coat applied by atmospheric plasma spray, Al_2O_3 thermally grown oxide (TGO), MCrAlY bond coat, and Ni-superalloy substrate.

Adopted from Clarke DR, Oechsner M, Padture NP. Thermal-barrier coatings for more efficient gas-turbine engines. MRS Bulletin 2012;37(10), 891–98. http://dx.doi.org/org/10.1557/mrs.2012.232.

essential to protect from heat. All of these layers have distinct mechanical, thermal, and physical properties that are mostly affected by thermal and mechanic conditions [24]. TBCs are used in turbine engine components such as turbine blades, combustors, combustor stationary guide vanes in the high-pressure section, and nozzles to obtain higher operating temperatures. For turbine systems they provide important advantages such as to increase the thrust to weight ratio, improve efficiency, decreased emission, and reduce air cooling. TBC systems contain either metal substrate features such as toughness, rigidity, and durability or ceramic material properties.

2.2.1 Ceramic Top Coat

TBCs are characterized by their closer thermal expansion coefficient with the substrate, low thermal conductivity, and high thermal gradient when exposed to flow of heat gases. The ceramic layer is located on top of the TBC system and influences hot gases and the high engine processing temperature. The ceramic top coat functions as an isolation layer to protect the metal substrate against a thermal effect and reduces the surface temperature. To reduce the surface temperature, the ceramic top layer

can be selected from a material with low thermal conductivity and an optimum thermal expansion coefficient. An increase in the thickness of the ceramic top coat can reduce heat transfer throughout the substrate. However, a thicker coating can create problems such as adhesion at the interface of the ceramic layer and bond coat and an increase in residual stress in the coating and a rise in the weight of the component. YSZ thermal barrier coatings can reduce the surface temperature at least about 50 to 80°C; when the operating temperature increases for 300-μm-thick ceramic coatings, the surface temperature can be reduced about 170 to 200°C [8,22].

2.2.2 Bond Coat

MCrAlY (M states Ni, Co or Ni and Co) has been widely used as a bond coat below a ceramic top coat in TBC systems. A bond coat can increase adherence between the ceramic top coat and substrate. It can also protect superalloy substrates from chemical attacks such as oxidation. Also, bond coats provide a reservoir from which Al can diffuse to form a protective α-Al_2O_3 TGO while protecting cohesion with the TBC without reacting with it. At the operating temperature, a bond coat should work to optimize cooling air from the substrate without reacting and melting. It should be advised that the bond coat temperature cannot exceed 1150°C. Bond coats are generally produced from metal alloys that can support TGOs. To achieve good adherence and minimize interdiffusion with the underlying superalloy, rare earth elements such Y and Hf (<1 wt%) can be added to the bond coat. The rare earth elements prominently increase the creep resistance of alumina ceramics [2,17,25,26].

The bond coat not only reduces the thermal expansion coefficient mismatch between the ceramic top coat and the substrate, it retards oxidation on the metallic substrate at a high temperature. High temperature application of TBCs causes the diffusion of oxygen through the ceramic top coat toward the bond coat. A TGO layer is formed on the bond coat. The TGO is a thin oxide layer (the thickness varies from 1 and 10 μ) that includes mainly Al_2O_3 and other oxides such as minor Cr_2O_3, NiO, and Ni $(Al, Cr)_2O_4$. The high ratio of mixed oxides on the interface can cause early spalling of the TBC [17,25,27]. Although this layer protects the substrate against further oxidation, the growth of TGO throughout thermal cycling and long-term exposure cause cracking and spallation of the ceramic top coat because of the thermal expansion mismatch between the oxide and metallic substrate. TGO scales on bond coatings can be affected by the thickness rate, bond coat surface roughness, hold time, and top coating composition. Increasing the TGO scale on the bond coat leads to stress at the interface. If this existing stress passes the strain tolerance of the TBC, destructive delamination can occur at the interface of the ceramic top coat. There are two main stresses in the TGO: one is related to growth strain as new oxide occurs at the grain boundaries of the TGO; the other is mismatch stress with the substrate formed by differences in thermal expansion upon cooling [28,29].

A uniform and dense α-Al_2O_3 oxide layer can hold off the formation of TGO during oxidation owing to ion diffusion, because α-Al_2O_3 is slow. The addition of Al_2O_3 into YSZ improves the thermomechanical properties of TBCs and decreases the thermal expansion top coat interface mismatch. Moreover, the existence of Al_2O_3 on the grain boundaries can provide the phase stability to YSZ. Rigid Al_2O_3 particles are not soluble within ZrO_2, and these particles surround the ZrO_2 particles, leading to compressive stress and decelerating the phase transformation of zirconia. It is not possible to use Al_2O_3 as a single ceramic top coat because the sprayed alumina contains Υ-Al_2O_3. It transforms into α-Al_2O_3 coupled with an increase in destructive volume of about 15% during thermal cycling [1,25].

Table 2 Chemical Composition of Inconel 718 Superalloy

Unit wt%	Ni	Cr	Mo	Co	W	Nb	Al	Ti	Fe	C
Inconel 718	53	19.06	3.04	0.11	–	5.08	0.52	0.93	18.15	0.021

2.2.3 Substrate Superalloys

Substrates are protected from the heat effect in TBC systems by powder coating. In TBCs, the system substrate is the essential part to protect from the heat effect. Superalloys have been improved for high-temperature operation, generally because high surface stability is required and relatively severe mechanical stress has been overcome. Superalloys are categorized as nickel base, cobalt base, and iron base. Ni-based superalloys are commonly used as substrates in gas turbines. Superalloys provide suitable matrix at high temperature and stress conditions in gas turbines and for a wide variety of other applications [2,29]. Superalloys work at high temperature and under rapid temperature changes and hard conditions such as stress. During operation they also undergo oxidation and corrosion, so all turbine components need to overcome these difficulties. This is why superalloys have been used as substrates for their high corrosion resistance, creep resistance, and fatigue resistance.

Most Ni-based superalloys include 10%−20% chromium, up to 8% aluminum and titanium, and 10%−20% cobalt. Usually small amounts of zirconium, beryllium, carbon molybdenum, tungsten, tantalum, hafnium, and niobium are added. Ni-based superalloys can be solid-solution strengthened, such as Haynes 230 and Hastelloy X, or precipitation hardened, such as Waspaloy and Inconel 738, 718, and 939 [30,31]. The chemical composition of the most common Ni-based alloy, Inconel 718, is given in Table 2.

Superalloys can preserve their durability at operating temperatures of about 1100°C, which is approximately 90% of the melting point of the superalloy. Moreover, fabrication methods such as forging, directionally solidified casting, and single crystal casting can affect the microstructure of the components and improve their mechanical properties at a higher temperature. Superalloys are produced in two different ways: are single crystal structure or directional grains; they have been used as substrate owing to their high creep resistance. The close-packed face-centered (cubic) structure of these alloys has creep, cracking, high-tensile, and thermomechanical fatigue properties that are much higher than equivalent body-centered cubic structures. Fig. 5 gives information about superalloys manufactured through different methods and the various operating temperatures of turbine components.

3. MANUFACTURING PROCESSES OF THERMAL BARRIER COATING

Manufacturing method directly effect microstructure of coatings. TBCs are manufactured using a variety of methods such as APS, EBPVD, HVOF, and suspension and solution plasma spray. APS, EBPVD, and HVOF are the most common methods for manufacturing TBCs because of their excellent properties. The manufacturing parameters are affected by the microstructure of the TBCs because of the operating time, thermomechanical resistance, and durability of the TBCs. A porous, defective, or lamellar microstructure in the plasma-sprayed coating can decrease the thermal conductivity of the YSZ about 60%. Porosity and cracks provide mechanical and thermomechanical adaptation in the TBC system during thermal cycling [8,9].

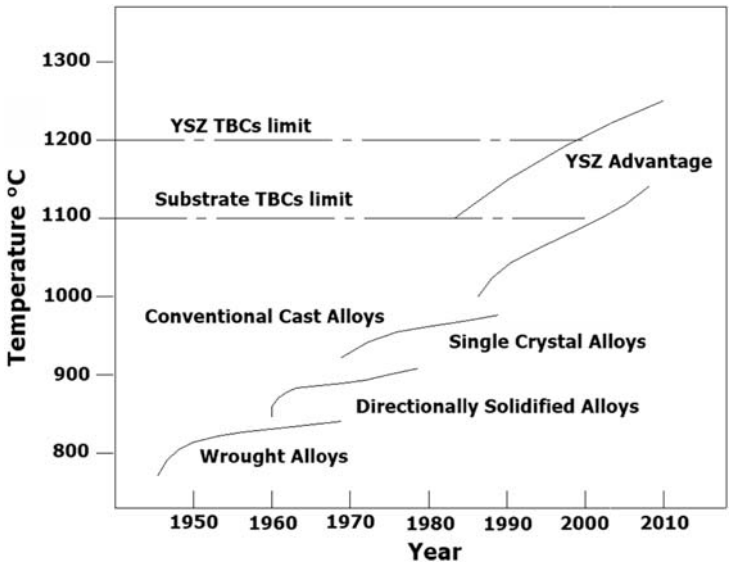

FIGURE 5

Effects of different fabrication processes of superalloys on operational temperatures. *TBC*, thermal barrier coating; *YSZ*, yttria-stabilized zirconia.

Adapted from Eriksson R. High-temperature degradation of plasma sprayed thermal barrier coating systems; 2011.

3.1 ELECTRON BEAM PHYSICAL VAPOR DEPOSITION

EBPVD was first used in the 1970s by Pratt and Whitney to deposit ZrO_2-Y_2O_3 on substrate. EBPVD is usually used to manufacture TBCs; many kinds of materials can be deposited with this method. EBPVD is expensive to implement in part because of the low efficiency with which materials are evaporated and the low deposition rate. In this method melting materials are evaporated under high pressure and then deposited onto the substrate. EBPVD also can provide a single crystal columnar microstructure with elongated intercolumnar voids aligned perpendicular to the substrate surface. The columnar microstructures include a small volume fraction of intercolumnar pores that are directed perpendicular to the coating interface. The column microstructures are excellent for their strong mechanical adhesion, smoother surface, high strain tolerance, ability to work under high operating temperatures, control of the microstructure of the deposited ceramics components, high flight working durability, and strong crystallographic texture. This method reduces thermal expansion mismatch stress and improves spallation resistance because of the columnar structure, which provides strain tolerance and better tensile strength. Because of these better properties, the method is usually preferred for gas turbine components that must work under hard mechanical and thermal conditions. The work area for the EBPVD method is limited in the space and aviation industry because to it needs high vacuum; thus, this increases the cost. A complex inner surface, rotating parts of aero engine components, and large components cannot deposit this method well. EBPVD TBCs provide aerodynamic stability in turbine blades and higher thermal shock resistance than APS during thermal cycling because of its columnar structure [32–34].

3.2 ATMOSPHERIC PLASMA SPRAY

APS TBCs are largely used as a main manufacturing method in gas turbine components to decrease the surface temperature, provide thermal insulation, and increase turbine productivity. Many materials can be deposited by this method because it can reach a high temperature above 10,000K. There are many benefits to APS TBCs in gas turbines, such as low cost, the longer operating time for the components, reduced stress in parts, a reduction in cooling air, lower emissions, high production performance, a large variety of coating thicknesses (30−1500 μm), and easy control of materials. APS TBCs have much better thermal isolation at operating temperature and show high oxidation resistance and prolonged service time. APS TBCs have higher thermal conductivity and limited chemical variability owing to vapor pressure issues, which are drawbacks coupled with low material deposition efficiencies of 2%−5% of evaporation. Feedstock type, plasma gas composition and substrate cooling, grain size, phase evolution, flow rate, energy input, and torch distance directly influence the microstructure of the coatings [35,36].

The plasma is generated by allowing a flow of argon, helium, or a similar gas between a tungsten cathode and a water-cooled copper anode. An electric arc is started between two electrodes using a high-frequency discharge, and then it continues using dc power. This arc heats the gas, which expands in the atmosphere forming a jet. The velocity at the nozzle's exit can reach 600−800 m/s. The molten or semimolten powder particles accelerate through the prepared substrate by the initial expansion of the gas and form the coating [16]. These powder particles solidify independently and quickly (108 K/s) as they crash a substrate or the surface. As a result, a complex microstructure can be formed that includes splat interfaces and incomplete regions, resulting in porosity. Typical APS ceramic coating porosity rates are range from 3% to 20%. Porosity inhibits the flow of heat through the substrate; consequently, it reduces the thermal conductivity of the coatings. APS coating microstructures can be summarized as layered structures built up via separated splats and porous. The lamella layered structure, another outstanding feature of plasma spray coating, has a large number of voids, pores of variable size and geometry. Their illustration, description, and scanning electron microscopy (SEM) image is given in Fig. 6.

Increasing porosity in TBCs can decrease residual stress that occurs in ceramic coatings because of a thermal expansion mismatch between the substrate and ceramic. Vertical cracks occur as a result of low adhesion between the lamellar microstructure and the bond coat or splats. These cracks can initiate when the coatings cool or at the low adhesive grain boundaries when high biaxial tensile residual stress is induced in the deposition surface. Horizontal and vertical cracks and the elasticity module in TBCs are key phenomena that affect the coating's performance. APS ceramic top coatings generally include many of microcracks. When the temperature increases, splats can transform into widescale macrocracks, which is called segmentation. It has been demonstrated that the scale of segmentation cracks rises at the expense of microspores as the substrate deposition temperature rises. When the segmentation cracks increase the stress tolerance of the coatings decrease. Fig. 7 compares the thermal conductivity value of APS TBCs and EBPVD TBCs. The APS YSZ coating has better thermal conductivity values at increased temperature than does the EBPVD TBC.

When both methods are compared, APS TBCs has many voids, cracks, and porosities because molten particles rapidly crashed onto the surface and solidified. Horizontal and porous microstructure of APS TBCs resulted in lower thermal conductivity and strength tolerance than those for the EBPVD TBCs. The surface roughness of EBPVD was better than APS TBCs. APS can provide a rich

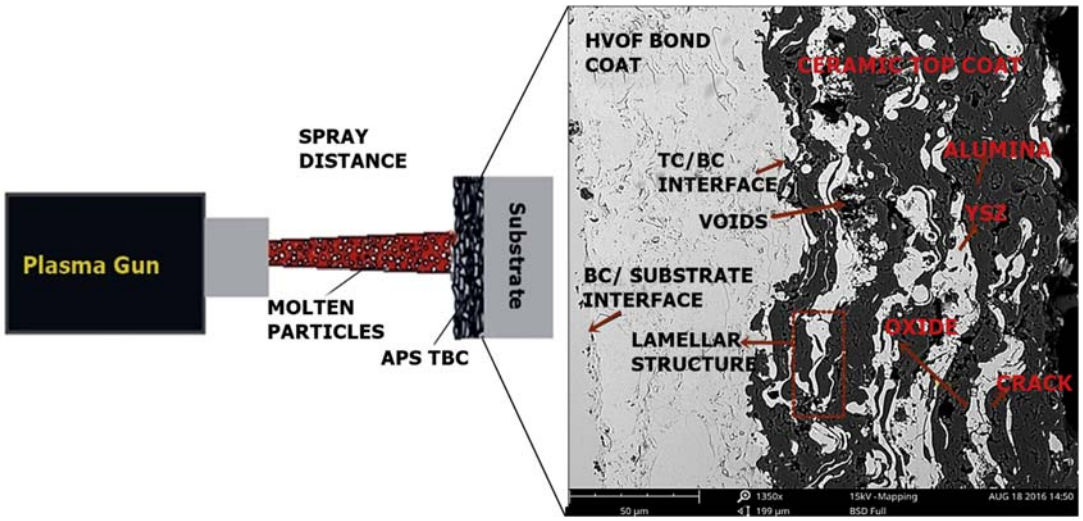

FIGURE 6

Illustration, description, and cross-section scanning electron microscopy image of atmospheric plasma spray (APS) thermal barrier coatings (TBCs). *BC*, bond coat; *HVOF*, high-velocity oxygen fuel; *TC*, top coat; *YSZ*, yttria-stabilized zirconia.

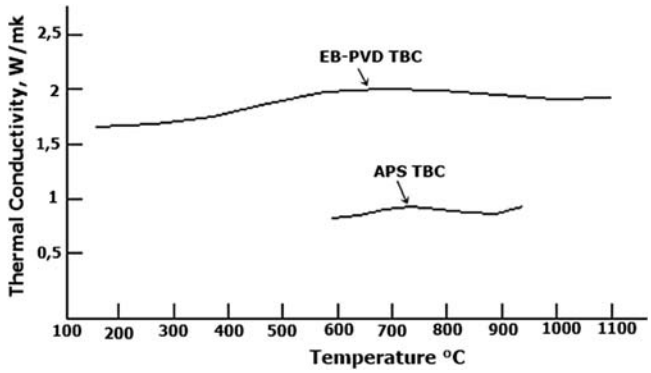

FIGURE 7

Thermal conductivity values of atmospheric plasma spray (APS) yttria-stabilized zirconia (YSZ) and electron beam physical vapor deposition (EB-PVD).

Adapted from AVCI A. Termal bariyer kaplamalarin oksidasyon ve sicaklik korozyonu davranişlarinin incelenmesi. Yildiz Technical University; 2014. Retrieved from: https://tez.yok.gov.tr/UlusalTezMerkezi/.

microstructure, flexible process and composition of coating materials. EBPVD has high quality microstructure low flexible process and high coating cost. Fig. 8 illustrates the microstructures of APS and EBPVD TBCs. The APS TBCs had 0.8−1.0 W/mK thermal conductivity at room temperature compared with EBPVD TBCs, which had much lower thermal conductivity, at 1.5−1.9 W/mK. The

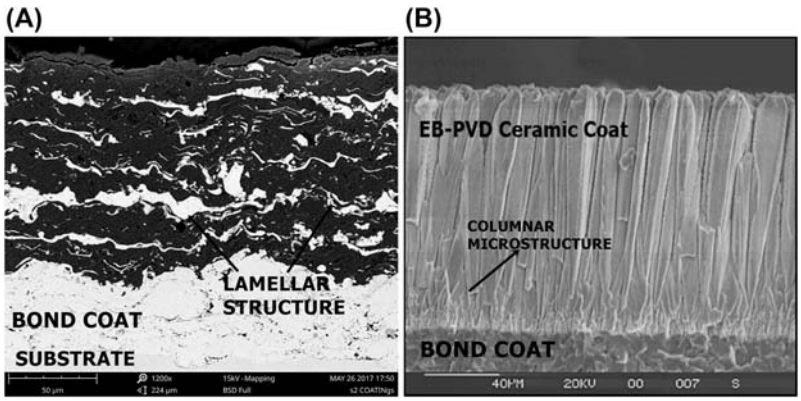

FIGURE 8

Scanning electron microscopy images of (A) atmospheric plasma spray (APS) thermal barrier coating, and (B) electron beam physical vapor deposition (EB-PVD) thermal barrier coating.

Adapted from AVCI, A. Termal bariyer kaplamalarin oksidasyon ve sicaklik korozyonu davranişlarinin incelenmesi. Yildiz Technical University; 2014. Retrieved from: https://tez.yok.gov.tr/UlusalTezMerkezi/.

rough surface was caused by oxygen diffusion through the bond coat; consequently, oxidation formed. At the high temperature, the substrate forced volume expansion to occur because of the lamellar microstructure. As a result of the APS TBCs, spallation or cracks were able to occur in the system. The deposition rate of APS was much more than for EBPVD and heating of the substrate was not necessary. EBPVD had a smoother surface, higher erosion resistance, and a columnar microstructure.

3.3 HIGH-VELOCITY OXYGEN FUEL

HVOF is thermal spray method developed in the 1980s by James Browning. In HVOF powder materials are generally applied, such as WC/Co, Cr_2C_3/NiCr, and dense cermet. HVOF is usually employed to deposit the bond coat owing to its outstanding coating properties such as high density, high adhesion, low oxide scale, and well-bonded ability to coat with a relatively high degree of accuracy. Because of its nature, it can be applied to large and complicated components cost-effectively. In HVOF, thermal spray powder materials are melted by a fuel and an oxygen mixture is burned, producing hot high-pressure stream. The powders exposure the flame in the combustion chamber; then they become molten or semimolten particles. The particles are fed into this high-pressure stream to spray toward the substrate. The particles' temperature range between 2300°C and 3000°C and the spraying speed can reach 1350 m/s. Fig. 9 shows a schematic diagram of the HVOF system.

Oxygen and fuel are fed into a combustion chamber where burning takes place. Burning gases vent through a torch gun passing through an 8- to 30-cm nozzle. The optimum spraying distance depends on the spray gun and the other equipment; it ranges between 220 and 380 mm. To burn oxygen, propane, natural gas, ethylene, and propylene can be used together. The coating microstructure can be affected by several parameters such as the oxygen−fuel mixture, which determines both the heat and spray velocity. The particle size also has a significant role in determining the coating structure. HVOF coatings have excellent wear, erosion resistance, and strong adhesion [37−41].

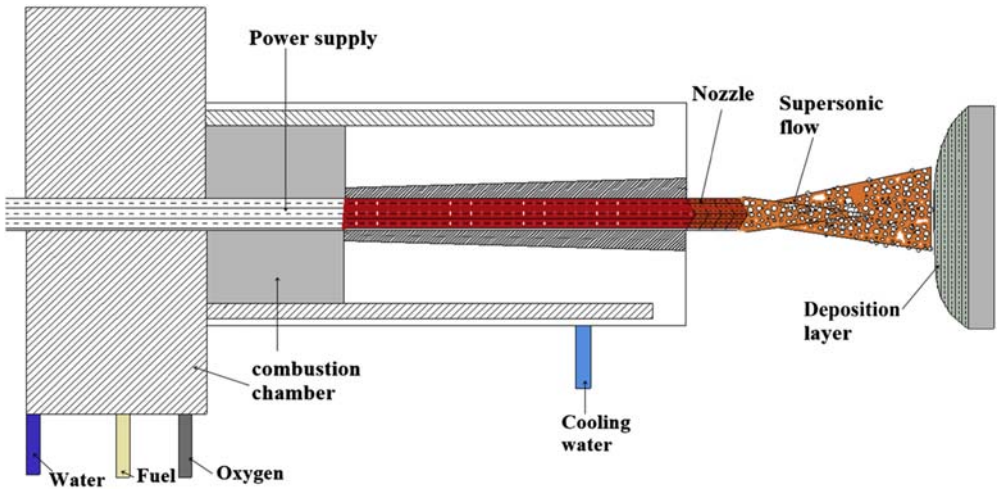

FIGURE 9

Schematic illustration of high-velocity oxygen fuel system.

4. FAILURE MECHANISMS AND PRECAUTIONS OF THERMAL BARRIER COATINGS

Various failures exist for TBCs, including thermal cycling mechanical forces in turbine engines, oxidation, hot corrosion, sintering of top coats, and thermal expansion coefficient mismatch between the ceramic top coat and metallic substrate. The most destructive failure mechanism is formation of the TGO layer in TBCs. Increase in the TGO scale causes the formation of stress in the TBC system due to heat transfers from thin bond coat to substrate. TGO formation leads to the consumption of Al in the bond coat. It can also cause the formation of different phases that cause to mismatch stress. The formation of TGO occurs as two types. If TBCs undergoes thermal cycling, the mechanism is shrinkage of TGO. However, if TBC undergoes an isothermal condition, the TGO grows. Sand particles in the environment can melt and react with TBCs during the takeoff and landing of aircraft (gas turbine temperatures can reach 1300°C). This melted sand is called calcia-magnesia-alumina-silicate (CMAS); it usually consists of magnesium oxide, calcium oxide, and aluminum oxide. CMAS was first distinguished in Warcraft engines by the US Army in the early 2000s. Researchers have tried to solve CMAS because it is an important problem related to the combustion temperature of gas turbine engines and it must be resolved before turbines can increase in performance from the increase in temperature. Fig. 10 gives examples of failure mechanisms and a ceramic top coat that has separated after thermal oxidation.

The purpose of laser is to have a smooth and dense surface to reduce a hot corrosion reaction and decrease CMAS and oxygen penetration. Studies showed that during thermal cycling, a TGO and thermal expansion coefficient mismatch between the metallic substrate and ceramic top coat leads to limited service time of TBCs. At a high temperature, oxygen diffuses through the bond coat as a result of porosity, roughness, and other microstructural defects of the ceramic top coat. Heat gases and a

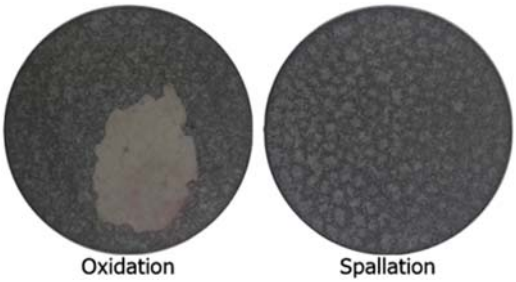

FIGURE 10

Failure mechanisms.

corrosive environment cause hot corrosion, erosion, and wear. Laser glazing remelts the rough surface and keeps solidification under control; as a result, a dense layer is formed on top of the TBCs. It has been shown that a network of vertical cracks in the coating created by laser glazing improves thermal shock resistance and thermal cycling. Studies reported that laser glazing treatment increases the service lifetime of TBCs about fourfold in hot corrosion; other studies reported increased oxidation resistance during thermal cycling. Laser glazing is limited to these defects [42–49].

5. EXPERIMENTAL STUDIES: OXIDATION

To increase the service lifetime of the coatings and improve the quality and durability of TBCs, specific tests were applied, such as oxidation, hot corrosion, and thermal shock. Oxidation occurs when a metal or alloy atoms leave their structure and then they react with oxygen. Oxidation also occurs in metallic elements of materials in oxygen or oxygen-containing atmospheres at high temperatures; these are then converted into their oxides. If materials are exposed to an oxygen-containing atmosphere over a long time, surface oxide forms like a sediment. Materials should show high surface stability to reduce materials lost during high-temperature oxidation. Oxidation causes a most destructive failure spallation, which result from cracks in TBC systems. The operating time of TBCs depends on the bond coat resistance against oxidation and corrosion at high temperatures. The inclusion of MCrAlY and Pt in the bond coat significantly affects the oxidation behavior and operating time of TBCs. Oxidation of the interface bond coat and top coat causes the formation of an oxide layer called TGO, which is a protective oxide layer consisting of alumina. If the bond coat supports enough (>3–5 wt%) Al to maintain a continuous Al_2O_3 layer, the TGO can become a protective layer. TGO also reduces oxygen diffusion through the substrate, so it protects the metal ions from oxygen. A decrease in aluminum occurs in the bond coat because aluminum is consumed by TGO and interdiffusion with a low aluminum substrate in a high operating temperature. TGO consists of aluminum oxide as well as other oxides such as some Cr_2O_3, NiO, and Ni $(Al, Cr)_2O_4$. To improve the operating service time of TBC systems, new-generation bond coats include a lot of Pt to obtain Υ-Ni + Υ'-Ni3Al. Bond coating with β-(Ni, Pt) provides no topologically close-packed phases and no impairing phase transformation [50].

This chapter aimed to compare oxidation resistance based on four different fabricated coatings: classical YSZ coatings, Al_2O_3, hybrid composite 50 wt% YSZ + Al_2O_3, and Al_2O_3/YSZ. To determine

the oxidation behavior and microstructural properties of TBCs at a high temperature, bond coats were deposited by HVOF and top coats were deposited by APS. AISI 304 stainless steel was used as a substrate in the shape of a disk (□25 × 4 mm). The sample's surface was grit blasted with alumina at a pressure of 6 bars and at 15 cm distance to remove oxides and improve adhesion between the substrate and the bond coat. Argon and hydrogen were the primary and secondary plasma gases, respectively. Commercial Metco Amdry 962 (Ni−22Cr− 10Al−Y) powder and was selected to deposit the bond coats and 204 NS (ZrO_2−8 wt% Y_2O_3) and 101NS (Al_2O_3), and their mixed different ratios were selected to be deposited as the ceramic top coat. Fig. 11 shows the steps taken to produce the TBCs and the morphology of the selected mixed powders.

Bond coats were deposited by HVOF using a commercial (Sulzer Metco) DJ-2700 gun and ceramic top coats were deposited by APS using APS 9 MBM plasma gun. Plasma guns were set on three-angle computer numerical control and the samples were placed on a rotating table, as shown in Fig 11. The specimens were taken into an air atmosphere electrical furnace for oxidation tests at 1050°C for 4 h and cooled in the furnace. Selected temperature was close the turbine operating temperature and phase transformation temperature of the YSZ. The stability of the coating was checked by looking for the appearance of any crack or spallation at the coating. Each result represented an average of three specimens and the average time to spallation was observed. The tests were stopped when the sample had any crack or spallation, and the time was recorded. The microstructures of sprayed coatings and those with oxidation were observed by SEM (Phenom World XL). The main reason for selecting AISI 304 was that it was able to preserve durability and strength at a high temperature, and it included Ni.

Fig. 12 shows macroscopic images after oxidation. The top coat of the YSZ and YSZ-Al_2O_3 samples lost some material during the oxidation test. However, overall spallation was observed in the Al_2O_3 and YSZ/Al_2O_3 samples owing to weak adhesion between bond coats. The A and Z50 A samples had low service time during the oxidation test at 1050°C. Failure occurred in the form of spallation from the bond coat because thermal stress formed in Al_2O_3 and it led to sudden spallation from the bond coat. Phase transformation from ɣ-Al_2O_3 to α-Al_2O_3 also may cause failure. Macroscopic images of the Z and ZA samples showed some spallation at the edge of the coatings. However, during thermal cycling a larger amount of TGO formed on the bond coat than on the A and ZA coatings.

The surface morphology of the APS TBCs samples was investigated by SEM. Dark regions on the top coat surface were Al_2O_3 and gray regions were YSZ (Fig. 13). APS TBCs had a lamellar structure

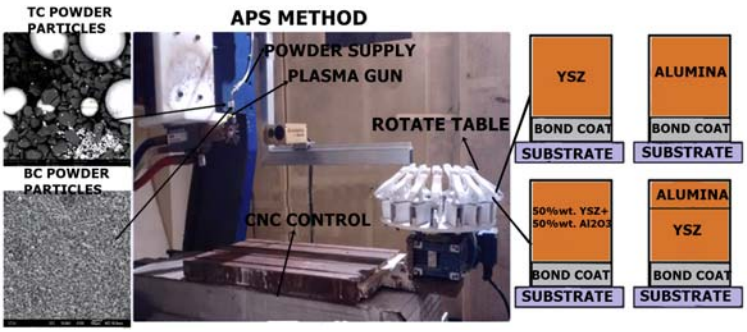

FIGURE 11

Production steps of atmospheric plasma spray (APS) thermal barrier coatings (TBCs). *BC*, base coat; *CNC*, computer numerical control; *TC*, top coat; *YSZ*, yttria-stabilized zirconia.

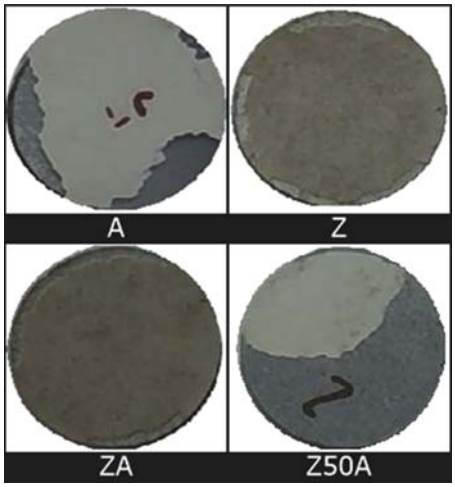

FIGURE 12

Macroscopic images of thermal barrier coatings after oxidation test.

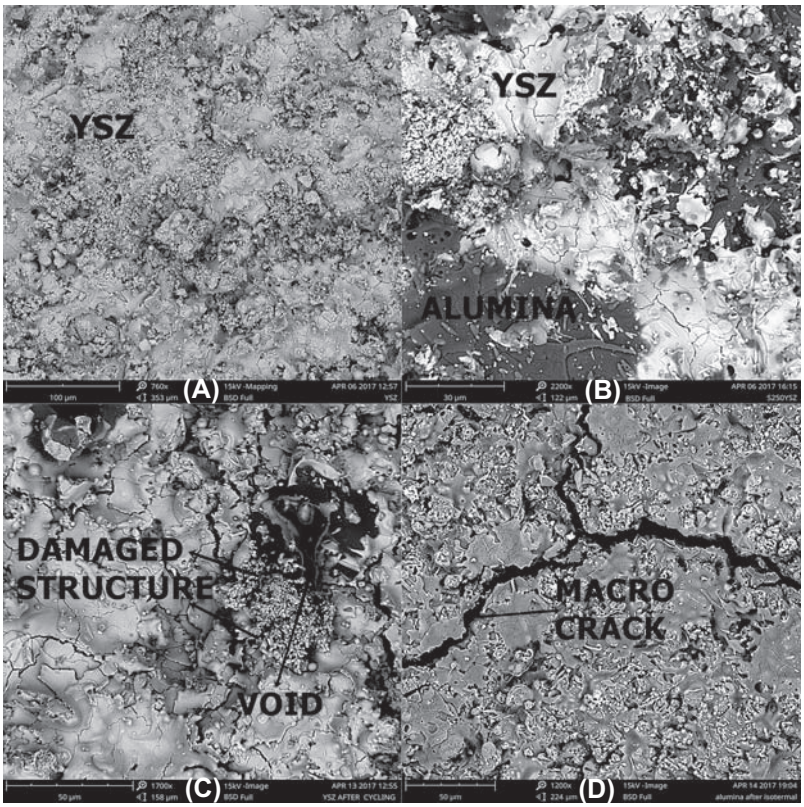

FIGURE 13

Surface scanning electron microscopy images of atmospheric plasma spray (APS) thermal barrier coatings; (A) APS yttria-stabilized zirconia (YSZ), (B) APS 50 wt% YSZ + 50 wt% Al_2O_3, (C) YSZ after oxidation, and (D) Al_2O_3 after oxidation.

with high porosity that transferred oxygen easily from the ceramic top coat to the metallic substrate and caused internal oxidation and destructive spallation. Macroscopic cracks and voids were investigated for the APS TBCs. In contrast, TGO not always protective when the TGO scale increased or a lower Al content in bond coat led an undesirable oxide top coat interface to form. The thickness of the ceramic coat was around 150 μm, and that of the bond coat was about 80 μm. The oxidation resistance of the TBC samples was in the order: YSZ, YSZ/Al_2O_3, Z50 A.

6. CONCLUDING REMARKS

The TBC system is used not only in the gas turbine industry but also as a significant material in gas turbines, land-based industrial gas turbines, shipboard engines, and diesel engines. Studies have focused on using bond coats, alternative top coat ceramics with low thermal conductivity. The selection of the material and the manufacturing methods can affect the service lifetime of TBCs. In the literature, there are many studies on the failure mechanisms of TBCs. In particular, studies have concentrated on the microscopic structure of TBCs, oxidation, thermal cycling, hot corrosion, and thermal shock behavior of TBCs. Even if these studies employed the same test, the application methods or parameters of those tests might be different. In this study, TBC coatings were produced by APS with high porosity. SEM investigation showed macroscopic cracks, voids, and an unmelted structure on top of the coatings. During oxidation tests, TGO formed at the interface of the bond coat and the top coat that led to the spallation of the top coat.

REFERENCES

[1] Dokur MM, Goller G. Processing and characterization of CYSZ/Al2O3 and CYSZ/Al_2O_3+YSZ multilayered thermal barrier coatings. Surface and Coatings Technology 2014;258:804−13. http://dx.doi.org/10.1016/j.surfcoat.2014.07.077.
[2] Clarke DR, Oechsner M, Padture NP. Thermal-barrier coatings for more efficient gas-turbine engines. MRS Bulletin 2012;37(10):891−8. http://dx.doi.org/10.1557/mrs.2012.232.
[3] Cao XQ, Vassen R, Stoever D. Ceramic materials for thermal barrier coatings. Journal of the European Ceramic Society 2004;24(1):1−10. http://dx.doi.org/10.1016/S0955-2219(03)00129-8.
[4] Limited WP. Thermal barrier coatings. Oxidation and hot corrosion of thermal barrier coatings (TBCs). In: Performance of thermal barrier coatings. woodhead; 2011. p. 356. Retrieved from www.knovel.com.
[5] Huibin X, veHong G. Thermal barrier coatings. limited. Sawston: W.P. Publishing; 2011. 302 pp.
[6] Sreedhar G, Alam MM, ve Raja VS. Hot corrosion behaviour of plasma sprayed YSZ/Al2O3 dispersed nicraly coatings on Inconel-718 superalloy. Surface and Coatings Technology 2009;204(3):291−9. http://dx.doi.org/10.1016/j.surfcoat.2009.07.026.
[7] Özgören Y. Stirling Motorunda termal Bariyer Kaplamanın Motor Performansına Etkilerinin Deneysel Olarak İncelenmesi. 2005. p. 122−33.
[8] Karaoglanli AC, Ogawa K, Türk A, Ozdemir I. Thermal shock and cycling behavior of thermal barrier coatings (TBCs) used in gas turbines. In: Progress in gas turbine performance; 2013. p. 237−60. http://dx.doi.org/10.5772/54412.
[9] Zhao H, Yu F, Bennett TD, Wadley HNG. Morphology and thermal conductivity of yttria-stabilized zirconia coatings. Acta Materialia 2006;54(19):5195−207. http://doi.org/10.1016/j.actamat.2006.06.028.
[10] Sudhangshu Bose, HT. High Temperature Coatings (n.d.).

[11] Witz G, Shklover V, Steurer W, Bachegowda S, Bossmann H-P. Phase evolution in yttria-stabilized zirconia thermal barrier coatings studied by rietveld refinement of X-ray powder diffraction patterns. Journal of the American Ceramic Society 2007;90(7820):2935−40. http://dx.doi.org/10.1111/j.1551-2916.2007.01785.

[12] Keyvani A, Saremi M, ve Sohi MH. Oxidation resistance of YSZ-alumina composites compared to normal YSZ TBC coatings at 1100°C. Journal of Alloys and Compounds 2011;509(33):8370−7. http://dx.doi.org/10.1016/j.jallcom.2011.05.029.

[13] Bengi T, Termal Bariyer Kaplamaların Isıl Özelliklerinin İncelenmesi Ve Düşük Termal İletkenlik İçin Parametre Optimizasyonu [Master thesis], Istanbul Technical University, Institute of Science and Technology.

[14] Saral U,ve Toplan N, YSZ Termal Bariyer Kaplamaların Mikroyapısal Ve Mekanik Özelliklerine Alümina İlavesinin Etkisi, The effect of Al_2O_3 addition on the microstructure and mechanical properties o YSZ thermal barrier coatings. VII. Ceramic Conference.

[15] Saral U. Alümina İlavesinin YSZ termal Bariyer Kaplamaların Mikro Yapı Üzerine Etkileri [Master thesis]. Sakarya: Sakarya University, Institute of Science and Technology; 2007.

[16] Saeidi S. Microstructure, oxidation & mechanical properties of as-sprayed and annealed HVOF & VPS CoNiCrAIY coatings [Thesis]. December 2011. Retrieved from: http://etheses.nottingham.ac.uk/1731/.

[17] Gao J, He Y, ve Wang D. Preparation of YSZ/Al2O3 micro-laminated coatings and their influence on the oxidation and spallation resistance of mcraly alloys. Journal of the European Ceramic Society 2011; 31(1−2):79−84. http://dx.doi.org/10.1016/j.jeurceramsoc.2010.08.010.

[18] Azhar AZA, Ratnam MM, ve Ahmad ZA. Effect of Al_2O_3/YSZ microstructures on wear and mechanical properties of cutting inserts. Journal of Alloys and Compounds 2009;478(1−2):608−14. http://dx.doi.org/10.1016/j.jallcom.2008.11.156.

[19] Özel S. Alüminyum alaşımı ve bronzu yüzeyine oksit ve karbür bileşiklerinin plazma sprey yöntemiyle kaplanmasının araştırılması [PhD thesis]. Elazıg University, Institute of Science and Technology; 2009.

[20] The American Ceramaic Society, editor. Progress in thermal barrier coatings. A. John Willey; 2008.

[21] Dalkılıç S. Bir termal Bariyer Kaplama Sisteminin Yorulma Davranışının İncelenmesi [PhD thesis]. Eskisehir: Anadolu University Institute of Science and Technology; 2007.

[22] Bhatia A. Thermal spraying technology and applications. 1999. p. 877.

[23] Çiftyürek E, %8 YSZ (İtriyum İle Stabilize Edilmiş ZrO_2) Termal Bariyer Kaplamaların (Tbk) Üretilmesi Ve Proses Parametreleri Optimizasyonu [Master thesis], Istanbul Technical University, Institute of Science and Technology, Istanbul.

[24] Kumar V, Balasubramanian K. Progress update on failure mechanisms of advanced thermal barrier coatings: a review. Progress in Organic Coatings 2016;90:54−82. http://dx.doi.org/10.1016/j.porgcoat.2015.09.019.

[25] Karaoglanli AC, Altuncu E, Ozdemir I, Turk A, ve Ustel F. Structure and durability evaluation of YSZ+Al_2O_3 composite tbcs with APS and HVOF bond coats under thermal cycling conditions. Surface and Coatings Technology 2011;205:S369−73. http://dx.doi.org/10.1016/j.surfcoat.2011.04.081.

[26] Wang S, Xu C, Ding Y, ve Zhang X. Thermal shock behavior of zrb2−sic composite ceramics with added tasi2. International Journal of Refractory Metals and Hard Materials 2013;41:507−16. http://dx.doi.org/10.1016/j.ijrmhm.2013.06.010.

[27] Saremi M, Afrasiabi A, ve Kobayashi A. Microstructural analysis of YSZ and YSZ/Al_2O_3 plasma sprayed thermal barrier coatings after high temperature oxidation. Surface and Coatings Technology 2008;202(14): 3233−8. http://dx.doi.org/10.1016/j.surfcoat.2007.11.029.

[28] Zhu C, Javed A, Li P, Yang F, Liang GY, Xiao P. A study of the microstructure and oxidation behavior of alumina/yttria-stabilized zirconia (Al_2O_3/YSZ) thermal barrier coatings. Surface and Coatings Technology 2012;212:214−22. http://dx.doi.org/10.1016/j.surfcoat.2012.09.052.

[29] Keyvani A, Saremi M, ve Heydarzadeh Sohi M. Microstructural stability of zirconia−alumina composite coatings during hot corrosion test at 1050°C. Journal of Alloys and Compounds 2010;506(1):103−8. http://dx.doi.org/10.1016/j.jallcom.2010.06.110.
[30] Eriksson R. High-temperature degradation of plasma sprayed thermal barrier coating systems. 2011.
[31] Giampaolo T. Gas turbine handbook, Principles and practices. 3rd ed. London: The Fairmont press, Inc.; 2006.
[32] Hass DD, Parrish PA, Wadley HNG. Electron beam directed vapor deposition of thermal barrier coatings. Journal of Vacuum Science & Technology A 1998. http://dx.doi.org/10.1116/1.581492.
[33] AVCI A. Termal bariyer kaplamalarin oksidasyon ve sicaklik korozyonu davranişlarinin incelenmesi. Yildiz Technical University 2014. Retrieved from, https://tez.yok.gov.tr/UlusalTezMerkezi/.
[34] Karabas M, Bal E, Taptık, İY. Effect of air plasma spray parameters on the properties of YSZ and CYSZ thermal barrier coatings. Journal of the Australian Ceramic Society 2016;52:175−82.
[35] Mishra SK, Pandey S, Mahato P, Kumar KS, Bysakh S, Sreemany M, ve Pathak LC. Microstructural studies on EB-PVD deposited nicraly, YSZ and lanthanum zirconate for thermal barrier applications. Surface and Coatings Technology 2012;207:143−8. http://dx.doi.org/10.1016/j.surfcoat.2012.06.045.
[36] Fitzpatrick R. The physics of plasmas. Ders Notları: Texas: The University of Texas at Austin; 2008. p. 6−7.
[37] Pierfrancesco R, Gianluca Z. PEEK biomaterials handbook. In: Kurtz SM, editor. Thermal plasma spray deposition of titanium and hydroxyapatite on polyaryletheretherketone implants (a volume in plastics design library); 2012. p. 119−42. Retrieved from: http://www.sciencedirect.com/science/book/9781437744637.
[38] Afrasiabi A, Saremi M, ve Kobayashi A. A comparative study on hot corrosion resistance of three types of thermal barrier coatings: YSZ, YSZ+ Al_2O_3 and YSZ/Al_2O_3. Materials Science and Engineering: A 2008; 478(1−2):264−9. http://dx.doi.org/10.1016/j.msea.2007.06.001.
[39] Yao R. Plasma-sprayed thermal barrier coatings with segmentation cracks (n.d.), 161−174.
[40] Keyvani A, Saremi M, Heydarzadeh M, Valefi Z, Yeganeh M, ve Kobayashi A. Microstructural stability of nanostructured YSZ − alumina composite TBC compared to conventional YSZ coatings by means of oxidation and hot corrosion tests. Journal of Alloys and Compounds 2014;600:151−8. http://dx.doi.org/10.1016/j.jallcom.2014.02.004.
[41] Saremi M, Valefi Z, ve Abaeian N. Hot corrosion, high temperature oxidation and thermal shock behavior of nanoagglomerated YSZ−Alumina composite coatings produced by plasma spray method. Surface and Coatings Technology 2013;221:133−41. http://dx.doi.org/10.1016/j.surfcoat.2013.01.038.
[42] Cao XQ, Vassen R, Tietz F, ve Stoever D. New double-ceramic-layer thermal barrier coatings based on zirconia−rare earth composite oxides. Journal of the European Ceramic Society 2006;26(3):247−51. http://dx.doi.org/10.1016/j.jeurceramsoc.2004.11.007.
[43] Faculty E. Evaluation of interface reactions in thermal barrier ceramic coatings. Surface and Coatings Technology 1997;97:361−5. http://dx.doi.org/10.1016/S0257-8972(97)00383-6.
[44] Thurn G, Schneider GAS, Aldinger F. High-temperature deformation of plasma-sprayed ZrO2, thermal barrier coatings institute. Materials Science 1997;5093(97).
[45] Bumgardner C, Croom BP, Li X. High-temperature delamination mechanisms of thermal barrier coatings: in-situ digital image correlation and finite element analyses. Submitted 2016;128:54−63. http://dx.doi.org/10.1016/j.actamat.2017.01.061.
[46] Zhang B, Wei L, Gao L, Guo H, Xu H. Microstructural characterization of PS-PVD ceramic thermal barrier coatings with quasi-columnar structures. Surface and Coatings Technology 2017;311:199−205. http://dx.doi.org/10.1016/j.surfcoat.2016.12.117.
[47] Leushakea U, Krella T, Schulz U, Peters M, Kayssera WA, Rabinb BH. Microstructure and phase stability of EB-PVD alumina and aluminalzirconia for thermal barrier coating applications. Surface and Coatings Technology 1997;95:131−6. http://dx.doi.org/10.1016/S0257-8972(97)00490-8.

[48] Levit M, Grimberg I, Weiss BZ. Residual stresses in ceramic plasma-sprayed thermal barrier coatings: measurement and calculation. Materials Science and Engineering: A 1996;206(1):30−8. http://dx.doi.org/10.1016/0921-5093(95)09980-8.

[49] Kokini K, Takeuchi YR, Choules BD. Surface thermal cracking of thermal barrier coatings owing to stress relaxation: zirconia vs. Mullite. Surface and Coatings Technology 1996;82(1−2):77−82. http://dx.doi.org/10.1016/0257-8972(95)02647-9.

[50] Brandl W, Toma D, Krüger J, Grabke HJ, Matthäus G. The oxidation behaviour of HVOF thermal-sprayed MCrAlY coatings. Surface and Coatings Technology 1997;94−95(97):21−6. http://dx.doi.org/10.1016/S0257-8972(97)00470-2.